Chinese Chemical Letters 34 (2023) 107740

Contents lists available at ScienceDirect

Chinese Chemical Letters

journal homepage: www.elsevier.com/locate/cclet

Silver-anchored porous aromatic framework for efficient conversion of propargylic alcohols with CO_2 at ambient pressure

Xiao-Xuan Guo[a,1], Zhao-Tian Cai[a,1], Yaseen Muhammad[b], Feng-Lei Zhang[c], Rui-Ping Wei[a], Li-Jing Gao[a], Guo-Min Xiao[a,*]

[a] School of Chemistry and Chemical Engineering, Southeast University, Nanjing 211189, China
[b] Institute of Chemical Sciences, University of Peshawar, 25120, KP, Pakistan
[c] Intelligent Transportation System Research Center, Southeast University, Nanjing 211189, China

ARTICLE INFO

Article history:
Received 19 April 2022
Revised 26 July 2022
Accepted 9 August 2022
Available online 11 August 2022

Keywords:
Porous aromatic framework
CO_2 capture
CO_2 conversion
α-Alkylidene cyclic carbonate
α-Hydroxy ketone

ABSTRACT

The conversion of propargylic alcohols and carbon dioxide (CO_2) into fine chemicals suffers from issues of harsh reaction conditions and difficult catalyst recovery. To achieve efficient CO_2 activation at low energy consumption, a silver-anchored porous aromatic framework catalyst Ag@PAF-DAB with high active phase density and CO_2 adsorption capacity was proposed. Since Ag@PAF-DAB has the dual functions of CO_2 capture and conversion, propargylic alcohols were completely converted into α-alkylidene cyclic carbonate or α–hydroxy ketone as high value-added product under atmospheric pressure (CO_2, 0.1 MPa) and low silver equivalent (0.5 mol%). Notably, Ag@PAF-DAB exhibited broad substrate diversity, high stability, and excellent reusability. By applying FTIR and GC, the key to green synthetic route of α–hydroxy ketone was confirmed to lie in the further hydration of α-alkylidene cyclic carbonate.

The utilization of CO_2 as a raw material to produce high value-added chemicals is a profitable strategy while concurrently diminishes the obnoxious environmental impacts by decreasing CO_2 concentration in the atmosphere [1,2]. However, CO_2 is an extremely stable molecule with a dissociation energy of 750 kJ/mol for the C=O bond, which is higher than other bonds such as C–H (430 kJ/mol) and C–C (336 kJ/mol) [3]. Therefore, the biggest obstacle to the large-scale production of important chemicals using CO_2 as a raw material is overcoming the high thermodynamic energy barriers and kinetic inertia to realize the conversion of CO_2. The synergistic activation of CO_2 with co-reagents (epoxides and nitrogen heterocyclic compounds *etc.*) is also crucial to achieve low energy consumption and high efficiency of CO_2 conversion. The intrinsic energy of these co-reagents provides the driving force that enhances the feasibility of CO_2 conversion [4].

Benefiting from the rapid development of green chemistry, scientists have developed various strategies to convert CO_2 into high value-added chemicals [5,6]. Among them, the carboxylative cyclization reaction of propargylic alcohols as a co-reagent and CO_2 to generate α-alkylidene cyclic carbonates has high atom economy with high market value of the final product [7,8]. Over the past decade, great efforts have been devoted to developing suitable catalytic systems for carboxylative cyclization reaction. Metal catalytic systems mainly include Ru [9], Ag [10], Pb [11], Cu [12], Zn [13] and K_2CO_3/crown ethers [14], as well as organic catalytic systems like N-heterocyclic carbenes [15], *N*–heterocyclic olefins [16] and bicyclic guanidines [17] have been reported. Although significant progress has been made, there are widespread issues with these methodologies such as harsh reaction conditions, difficult catalyst recovery, and poor product selectivity. Therefore, the design of efficient and recyclable catalysts for CO_2 carboxylative cyclization remains a challenge.

At present, porous aromatic framework materials (PAFs), as a kind of important organic polymer materials, have attracted great interest of researchers due to their high CO_2 adsorption capacity, excellent chemical tunability and outstanding stability [18,19]. PAFs not only serve as suitable carriers of metal active site but also effectively couple CO_2 capture and conversion. Inspired from these intriguing properties, herein, we report a silver based porous aromatic framework-3,3′-diaminobenzidine (Ag@PAF-DAB) catalyst with high active phase density and CO_2 adsorption capacity (Scheme 1a). Firstly, PAF-DAB was synthesized by efficient assembly of DAB (3,3′-diaminobenzidine) as building blocks through oxidative coupling reaction. Then, the azo functional groups of acted as stabilizers for the growth of Ag, ensuring that the Ag nanoparticles uniformly dispersed on PAF-DAB and maintained

* Corresponding author.
E-mail address: xiaogm426@gmail.com (G.-M. Xiao).
[1] These authors contributed equally to this work.

https://doi.org/10.1016/j.cclet.2022.08.020
1001-8417/

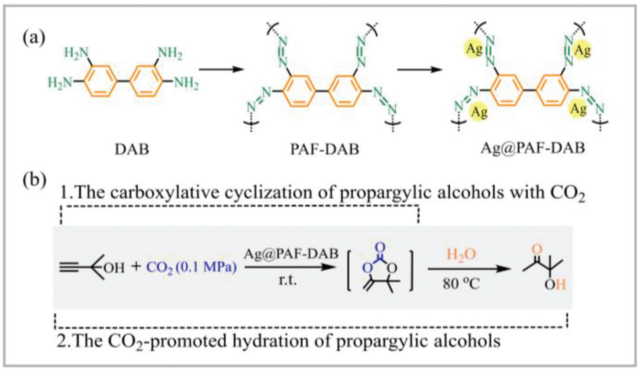

Scheme 1. (a) Schematic illustration for the synthesis of Ag@PAF-DAB. (b) Transformation of propargylic alcohols into α-alkylidene cyclic carbonate and α–hydroxy ketone.

suitable sizes. Since the structure of PAF-DAB contains rigid aromatic group units connected by C–C bonds, thus it exhibits ultrahigh specific surface area (SSA) and excellent stability [20]. The high active phase density and CO_2 adsorption capacity endows Ag@PAF-DAB with excellent catalytic activity and selectivity in the carboxylative cyclization of propargylic alcohols and CO_2 under ambient reaction conditions. Interestingly, a high-value-added product, *i.e.*, α–hydroxy ketone, was obtained in high yield at 80 °C and adding 2 equiv. H_2O in the original carboxylative cyclization reaction. The results show that Ag@PAF-DAB can be concomitantly and efficiently applied in the two reaction systems and hence enhances its broad-spectrum applications for large-scale applications (Scheme 1b).

Firstly, the PAF-DAB was synthesized by DAB monomer under the oxidative action of (diacetoxyiodo)benzene [21]. Then, Ag@PAF-DAB catalysts were obtained after introducing high catalytic activity phase "Ag" into the framework, which contains rich azo groups. The Ag@PAF-DAB catalyst could be stored in air for a long time and is insoluble in water or general organic solvents such as DCM and DMF, proving that the catalyst has a highly stable cross-linked structure. In the solid-state ^{13}C NMR spectrum of PAF-DAB (Fig. S1 in Supporting information), a series of strong signals are observed at the chemical shifts of 110–155 ppm. Compared with the ^{13}C NMR spectrum of DAB (Fig. S2 in Supporting information), it can be seen that these peaks are attributed to aromatic carbon of benzene ring, indicating that the raw material components DAB are successfully combined into polymerization network [21]. As shown in Fig. 1a, the stretching vibration peak ($\nu = 3380$ cm^{-1}) and bending vibration peak ($\nu = 1637$ cm^{-1}) are assigned to primary amine N–H [22]. These characteristic peaks disappeared in the aromatic skeleton of PAF-DAB, while a new absorption peak appeared at $\nu = 1410$ cm^{-1}, which was attributed to the stretching vibration peak of –N=N–, demonstrating the successful coupling and polymerization of monomer through -NH_2 groups oxidation [23]. PAF-DAB has no diffraction peaks and presents an amorphous state as observed by PXRD pattern (Fig. 1b). However, there are obvious diffraction peaks at 38.1°, 44.2°, 64.5°, 77.5° in Ag@PAF-DAB after loading Ag, which correspond to the standard PDF card of Ag(0) (JCPDS: No. 89–3722) [24]. These results provide sufficient evidence that the active center Ag in the catalyst mainly exists in the form of elementary substance.

In the full survey XPS spectra, it can be seen that PAF-DAB and Ag@PAF-DAB are consistent with the raw material components (Fig. S3 in Supporting information). Specifically, in the N 1s XPS spectra (Fig. 1c), the DAB monomer shows a signal at the binding energy (BE) of 398.4 eV, which is ascribed to N atom in –NH_2 [25]. This signal weakened significantly after the coupling, and a new signal appeared at the BE = 399.2 eV, which was attributed to

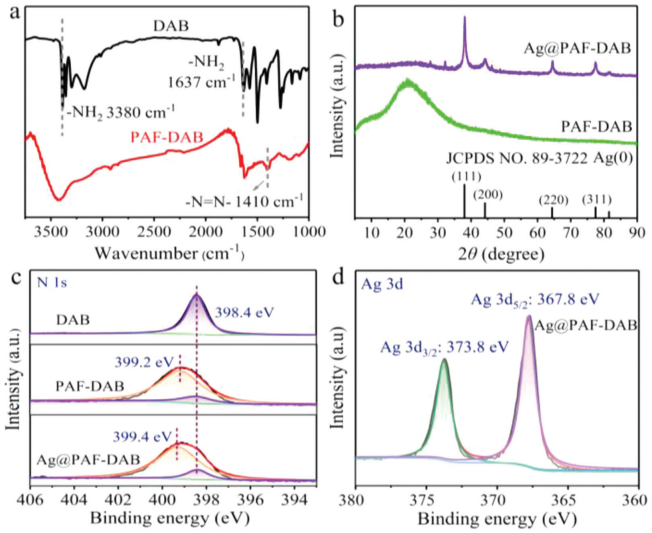

Fig. 1. (a) FT-IR spectra of DAB and PAF-DAB. (b) XRD patterns of PAF-DAB and Ag@PAF-DAB. (c) N 1s and (d) Ag 3d XPS spectra of Ag@PAF-DAB.

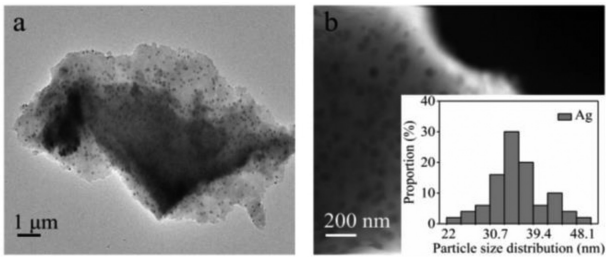

Fig. 2. (a) TEM image of Ag@PAF-DAB. (b) Particle size distribution of Ag.

N atom in –N=N–, confirming that –NH_2 was successfully bonded to form an azo group under oxidation environment [26]. After the coordination of Ag and azo group, the electron cloud density of N decreased and BE increased to 399.4 eV. Fig. 1d indicate that the BE positions of Ag $3d_{5/2}$ and Ag $3d_{3/2}$ in Ag@PAF-DAB appeared at 367.8 eV and 373.8 eV, which were consistent with the reported signal of Ag element, indicating the active elemental Ag center was successfully incorporated into the aromatic skeleton [27]. In addition, the content of Ag element in the catalyst was determined to be 7.26% by ICP-OES which is close to the theoretical value.

It is evident from SEM image (Fig. S4a in Supporting information) that Ag@PAF-DAB presents a micron-scale amorphous lumped structure, and the elemental distribution diagrams show that polar heteroatoms N and active center Ag are uniformly distributed on the aromatic framework (Figs. S4b and S5 in Supporting information). It was observed from TEM analysis that the loaded Ag nanoparticles on the aromatic framework were uniform in size and distribution, with a particle size of about 35 nm (Figs. 2a and b). Moreover, adsorption-desorption experiments were carried out with N_2 as the probe molecule at 77 K to conduct the SSA and pore size distribution of the aromatic framework materials. Fig. S6 (Supporting information) shows that their N_2 adsorption-desorption isotherms belong to typical I-type curves [28], and the SSA of PAF-DAB is 753.4 m^2/g. The SSA of Ag@PAF-DAB was slightly reduced to 561.9 m^2/g after Ag loading, which is attributed to the coverage by metal [29], but the pore size remained unchanged at 0.59 nm (Fig. S7 in Supporting information). These results reveal that the aromatic skeleton catalyst exhibits high SSA and plentiful pore structure, which is beneficial to the efficient mass/heat transfer during the catalytic reaction. Fig. S8 (Supporting information) shows that the CO_2 adsorption amount is as high as 3.21 mmol/g at 273 K

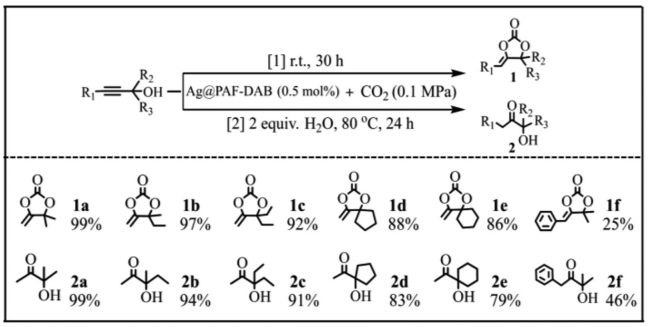

Fig. 3. Results of the carboxylative cyclization and hydration of other propargylic alcohols with CO_2 over Ag@PAF-DAB. Reaction: substrate (2 mmol), catalyst amount equal to the amount of Ag, DBU (1 equiv.), MeCN (4 mL). Determined by GC using naphthalene as an internal standard.

and 0.1 MPa, and the adsorption amount remained at 1.98 mmol/g at 298 K and 0.1 MPa. The CO_2 equivalent heat of adsorption of Ag@PAF-DAB was 36.2 kJ/mol under low CO_2 coverage according to the Clausius-Clapeyron equation [30]. This higher value demonstrates that the N-rich porous aromatic framework has a strong physical adsorption effect on CO_2, corresponding to the previous results of high CO_2 adsorption [31,32]. Based on the above analysis, it can be predicted that the highly dispersed metal active centers and CO_2 adsorption will greatly intensify the subsequent CO_2 catalytic conversion.

After the synthesis and characterization of Ag@PAF-DAB catalyst, its catalytic performance in the carboxylative cyclization reaction of propargylic alcohols with CO_2 was investigated at room temperature and pressure. 2-Methyl-3-butyn-2-ol was selected as the model substrate and DBU (1,8-diazabicyclo[5.4.0]undec–7-ene, 1 equiv.) was used as an effective base additive for the carboxylative cyclization reaction. The experiment was carried out according to the general procedure of the conversion reaction of propargylic alcohols and CO_2. The results indicated that in the absence of catalyst or 0.5 mol% PAF-DAB catalyst in the system, no product was generated after 36 h of reaction (Table S1 in Supporting information). When 0.5 mol% Ag@PAF-DAB was added, a nearly complete yield of α-alkylidene cyclic carbonate was obtained within 30 h (Fig. S9 in Supporting information). Compared with Ag-based catalysts previously reported, this amount of catalyst is much less [24,33-38], which is also a rare CO_2 conversion reaction under these conditions, as shown in Table S2 (Supporting information). The high efficiency of Ag@PAF-DAB is attributed to the construction of the polymer framework that provides a microenvironment which is conducive for the reaction. At the same time, the high and uniform distribution of the Ag active center facilitates the proximity of the substrates, thus improving the reaction efficiency.

Encouraged by the successful experimental results, Ag@PAF-DAB was applied for the hydration reaction of propargylic alcohol. The experimental procedure was the same as that for carboxylative cyclization, except that additional H_2O (2 equiv.) and raising reaction temperature to 80 °C. Similarly, no product was generated in the absence of active center Ag(0) or CO_2 in the blank experiment (Table S3 in Supporting information). However, under the catalysis of 0.5 mol% Ag@PAF-DAB, propargylic alcohol was completely converted within 24 h to generate another high value-added product *i.e.*, α–hydroxy ketone (Fig. S10 in Supporting information). In addition, the Ag@PAF-DAB system was still extended in the conversion of various types of substrates, including aliphatic chain-substituted, aliphatic-ring-substituted, and aromatic-ring-substituted substrates (Fig. 3). Apparently, the difficulty of catalytic conversion of substrates depends on steric hindrance effect of substrate substituents [39]. When the substrate substituent was methyl (**1a** and **2a**), ethyl (**1b** and **2b**), diethyl (**1c** and **2c**) and other groups with less steric hindrance, the target product was obtained in high yield in a short time. When the substituents of the substrate were cyclopentyl (**1d** and **2d**) and/or cyclohexyl (**1e** and **2e**), the yield of the target product decreased significantly. In addition, the catalytic substrates were not limited to terminal propargylic alcohols, but also exhibited certain catalytic activity for endopropargylic alcohols (**1f** and **2f**). These findings thus concluded that Ag@PAF-DAB exhibits catalytic diversity and remarkable functional group tolerance and hence has a wide application prospect.

The recycling performance of catalysts is an important index to evaluate the stability of catalysts. The reusability of Ag@PAF-DAB was separately investigated in carboxylative cyclization and hydration reactions. The catalyst was reused directly in the next cycle after simply filtering, washing and drying. It is worth noting that since the collection process caused a small loss of catalyst, fresh catalyst (<15 wt%) was supplemented in the second and third cycle to ensure that the amount of catalyst was 0.5 mol%. According to Fig. S11 (Supporting information), Ag@PAF-DAB catalyzed the above two model reactions with high conversion (>80%) for three successive reuses. Among them, the cycle performance decreased after the first cycle caused by Ag content loss (6.51%) in the long carboxylative cyclization reaction time. The ICP-OES analysis results showed that the Ag content of the reused Ag@PAF-DAB catalyst after three cycles in the two reactions was 6.23% and 6.84%, respectively, which was slightly lower than that of the fresh catalyst. Moreover, PXRD tests were performed on Ag@PAF-DAB(I) and Ag@PAF-DAB(II) and the results revealed that the PXRD pattern of reused catalyst realized minimal changes (Fig. S12 in Supporting information), thereby confirming the high stability of the catalyst. These results conclude that Ag@PAF-DAB could efficiently balance catalyst dose minimization and stability by its excellent recyclability and hence can be deemed of great promise for practical applications.

The reaction mechanism was further explored. Firstly, signal peak of hydroxyl group was detected by ^{1}H NMR spectroscopy (Fig. S13 in Supporting information). Propargylic alcohol showed a sharp single peak at $\delta = 5.28$ ppm, which was attributed to the H atom signal peak in the alcoholic hydroxyl group. However, in the propargylic alcohol/DBU system, the signal peak of H changed to a wide peak, indicating that DBU could activate the hydroxyl group of propargylic alcohol to facilitate subsequent CO_2 insertion into −O···H. In addition, real time FT-IR and GC analyses were used to monitor the reaction process. The FR-IR spectra detected that the stretching vibration peaks of C=O ($\nu = 1825$ cm^{-1} and 1685 cm^{-1}) and C−O ($\nu = 1172$ cm^{-1} and 1034 cm^{-1}) got gradually clearer and sharper with the accumulation of time within 240 min of the reaction, confirming the process of CO_2 activation and insertion (Fig. 4a). It was further confirmed by the GC spectrum that propargylic alcohol was gradually converted into α-alkylidene cyclic carbonate. Moreover, the presence of DBU causes the chemical shift of the H atom in H_2O to the downfield by ^{1}H NMR spectroscopy, which is due to their hydrogen bond association [40]. It indicates that DBU can directly activate H_2O molecules (Fig. S14 in Supporting information). After adding water, the FT-IR spectrum monitored the stretching vibration peaks belonging to C=O and C−O gradually broadened and disappeared within 240–360 min, corresponding to the decarboxylation of α-alkylidene cyclic carbonate and the release of CO_2 (Fig. 4b). Meanwhile, the GC spectrum showed that α-alkylidene cyclic carbonate was converted into α–hydroxy ketone as the final product within this time period (Fig. 4c). It can be seen that the key to the synthesis path of α–hydroxy ketone lies in the further hydration of the intermediate (α-alkylidene cyclic carbonate). Based on the experimental results and previous literature reports [34,41], we proposed the possible route for the carboxyla-

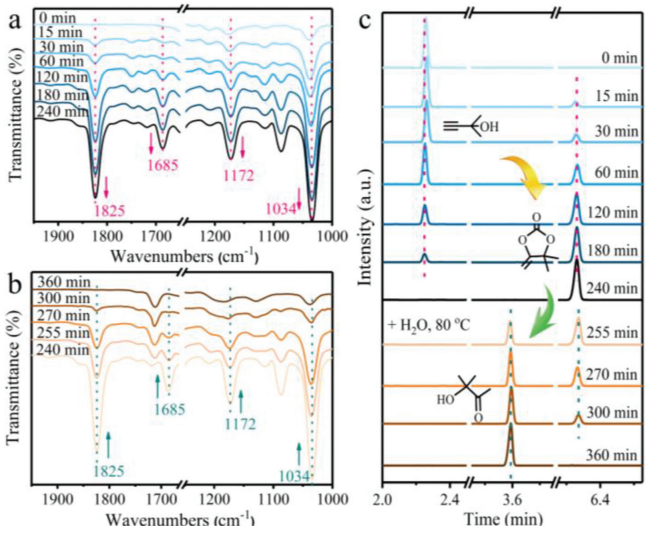

Fig. 4. (a) FT-IR spectra of the carboxylative cyclization reaction system. Reaction: 2-methyl-3-butyn-2-ol (6 mmol), Ag@PAF-DAB (4 mol%), DBU (1 equiv.), MeCN (12 mL), CO_2 (0.1 MPa), 40 °C, 1 mL reaction mixture was collected for detection every time. (b) FT-IR spectra of the hydration reaction system. Reaction: 80 °C, H_2O (2 equiv.). (c) GC patterns of the carboxylative cyclization and hydration reaction system.

tive cyclization and hydration of propargylic alcohols with CO_2 catalyzed by Ag@PAF-DAB system as shown in Fig. S15 (Supporting information). Incipiently, the complex **1** is generated by the coaction of Ag@PAF-DAB, propargylic alcohol and DBU. The activated alcoholic hydroxyl group of the substrate further captures CO_2 with the assistance of organic framework to generate carbaminate adduct **2**. Subsequently, the carbaminate rapidly attacks the activated alkynyl group, resulting in intramolecular cyclization to obtain the vinyl intermediate **3**. The generated five-membered ring undergoes protonation to obtain the target product α-alkylidene cyclic carbonate, and dissociates Ag@PAF-DAB and DBU to participate in the next catalytic cycle. In addition, the α-alkylidene cyclic carbonate will further react in the presence of water. Water acts as a nucleophile in the presence of DBU to attach the carbonyl group, leading to the opening of the five-membered ring to generate intermediate **4**. Finally, intermediate **4** is decarboxylated and tautomerized to obtain α–hydroxy ketone.

Based on the above analysis, a porous aromatic framework catalyst Ag@PAF-DAB was designed and synthesized through oxidative coupling reaction. The flexible framework and abundant polar nitrogen atoms endowed Ag@PAF-DAB with strong CO_2 affinity and high CO_2 adsorption capacity (3.21 mmol/g, 273 K, 0.1 MPa). Due to the synergistic properties of CO_2 capture and activation, Ag@PAF-DAB achieves efficient catalytic carboxylative cyclization and hydration of propargylic alcohols under atmospheric conditions. In addition, Ag@PAF-DAB as a heterogeneous catalyst also exhibited excellent reusability, high catalytic diversity, and outstanding substrate universality. Overall, this work provides an important reference for the further development of a highly integrated chemical process that combine CO_2 capture and utilization.

Declaration of competing interest

The authors declare that they have no known competing financial interests or personal relationships that could have appeared to influence the work reported in this paper.

Acknowledgment

This study was supported by the National Key Research and Development Program of China (No. 2019YFB1504003).

Supplementary materials

Supplementary material associated with this article can be found, in the online version, at doi:10.1016/j.cclet.2022.08.020.

References

[1] R. Xu, H. Xu, S. Ning, et al., Trans. Tianjin Univ. 26 (2020) 470–478.
[2] S. Wu, J. Wang, Q. Li, et al., Trans. Tianjin Univ. 27 (2021) 155–164.
[3] T.R. Chen, F.S. Wu, H.-P. Lee, et al., J. Am. Chem. Soc. 138 (2016) 3643–3646.
[4] R. Calmanti, M. Selva, A. Perosa, Green Chem. 23 (2021) 1921–1941.
[5] G. Bharath, K. Rambabu, A. Hai, et al., Appl. Catal. B 298 (2021) 120520.
[6] P. Yaashikaa, P.S. Kumar, S.J. Varjani, et al., J. CO_2 Util. 33 (2019) 131–147.
[7] Z.Z. Yang, Y. Zhao, H. Zhang, et al., Chem. Commun. 50 (2014) 13910–13913.
[8] R. Das, C. Nagaraja, Green Chem. 23 (2021) 5195–5204.
[9] C. Bruneau, P.H. Dixneuf, J. Mol. Catal. 74 (1992) 97–107.
[10] S.S. Islam, S. Biswas, R.Ali Molla, et al., ChemNanoMat 6 (2020) 1386–1397.
[11] K. Iritani, N. Yanagihara, K. Utimoto, J. Org. Chem. 51 (1986) 5499–5501.
[12] H.S. Kim, J.W. Kim, S.C. Kwon, et al., J. Organomet. Chem. 545 (1997) 337–344.
[13] V. Panwar, S.L. Jain, J CO_2 Util. 24 (2018) 306–314.
[14] K. Uemura, T. Kawaguchi, H. Takayama, et al., J. Mol. Catal. A: Chem. 139 (1999) 1–9.
[15] Y. Kayaki, M. Yamamoto, T. Ikariya, Angew. Chem. 121 (2009) 4258–4261.
[16] Y.B. Wang, Y.M. Wang, W.Z. Zhang, et al., J. Am. Chem. Soc. 135 (2013) 11996–12003.
[17] N.D. Ca', B. Gabriele, G. Ruffolo, et al., Adv. Synth. Catal. 353 (2011) 133–146.
[18] Y. Tian, G. Zhu, Chem. Rev. 120 (2020) 8934–8986.
[19] Y. Yuan, F. Sun, L. Li, et al., Nat. Commun. 5 (2014) 1–8.
[20] R. Li, G. Xing, H. Li, et al., Chin. Chem. Lett. 34 (2023) 107454.
[21] J. Wang, Y. Zhang, et al., Green Chem. 18 (2016) 5248–5253.
[22] T. Ramanathan, F. Fisher, R. Ruoff, et al., Chem. Mater. 17 (2005) 1290–1295.
[23] K. Su, W. Wang, B. Li, et al., ACS Sustain. Chem. Eng. 6 (2018) 17402–17409.
[24] D. Chakraborty, P. Shekhar, H.D. Singh, et al., Chem. Asian J. 14 (2019) 4767–4773.
[25] X. Fang, S. Wu, Y. Wu, et al., Appl. Surf. Sci. 518 (2020) 146226.
[26] O. Oloye, J.D. Riches, A.P. O'Mullane, Chem. Commun. 57 (2021) 9296–9299.
[27] H.J. Li, A.Q. Zhang, Y. Hu, et al., Nanoscale Res. Lett. 7 (2012) 1–13.
[28] D. Shan, J. Yang, W. Liu, et al., J. Mater. Chem. A 4 (2016) 13589–13602.
[29] S. Subhan, A.U. Rahman, M. Yaseen, et al., Fuel 237 (2019) 793–805.
[30] L. Zou, Y. Sun, S. Che, et al., Adv. Mater. 29 (2017) 1700229.
[31] P. Puthiaraj, S. Ravi, K. Yu, et al., Appl. Catal. B 251 (2019) 195–205.
[32] J.H. Zhu, Q. Chen, Z.Y. Sui, et al., J. Mater. Chem. A 2 (2014) 16181–16189.
[33] Z. Zhou, C. He, L. Yang, et al., ACS Catal. 7 (2017) 2248–2256.
[34] Q.W. Song, B. Yu, X.D. Li, et al., Green Chem. 16 (2014) 1633–1638.
[35] K. Chen, G. Shi, R. Dao, et al., Chem. Commun. 52 (2016) 7830–7833.
[36] G. Shi, R. Zhai, H. Li, et al., Green Chem. 23 (2021) 592–596.
[37] G. Zhang, H. Yang, H. Fei, ACS Catal. 8 (2018) 2519–2525.
[38] X. Wang, W. Li, J. Wang, et al., Dalton Trans. 49 (2020) 13052–13059.
[39] Y. Yuan, Y. Xie, C. Zeng, et al., Green Chem. 19 (2017) 2936–2940.
[40] H. Koller, G. Engelhardt, R.A. Van Santen, Top. Catal. 9 (1999) 163–180.
[41] H. He, C. Qi, X. Hu, et al., Green Chem. 16 (2014) 3729–3733.